Supporting Information

Improving the Development of Human Engineered Cardiac Tissue by Gold Nanorods Embedded Extracellular Matrix for Long-Term Viability

Alberto Sesena-Rubfiaro[1], Navin J. Prajapati[1], Lihua Lou[2], Govinda Ghimire[1], Arvind Agarwal[2] and Jin He[1,3*]

[1]Department of Physics, Florida International University, Miami, FL 33199, USA

[2]Department of Mechanical and Materials Engineering, Florida International University, Miami, FL 33174, USA

[3]Biomolecular Science Institute, Florida International University, Miami FL 33199, USA

*corresponding author

This PDF file includes: Figures S1-S6

Videos for Figure S3 and S5 are also available.

Contents

S1. Materials and methods

Immunofluorescence imaging of sarcomere structure

The tissues were fixed with 4% paraformaldehyde in PBS and permeabilized with 0.2% Triton X-100 in PBS for 40 min. Then, the tissues were rinsed in PBS for 5 min and incubated in blocking solution 1% bovine serum albumin (BSA) in PBS for 1 h. The tissues were incubated overnight with primary antibody anti-sarcomeric α-actinin (mouse monoclonal, 1:200; Abcam ab9465) diluted in 1% BSA. On the next day, the tissues were rinsed for 5 min in PBS and incubated with a secondary antibody for 2 h: anti-mouse IgG–Alexa Fluor 488 (1:400; Invitrogen A21202). Subsequently, the hECTs were incubated for 10 min with 4', 6-diamidino-2-phenylindole (DAPI, Invitrogen, 30 nM) and rinsed in 1xPBS for 5 min. Fluorescence images were acquired using a Nikon C1 confocal microscope equipped with a 60x objective and Nikon NIS Elements software. At least three regions of interest (ROIs) were imaged per biological replicate and three biological replicates were used for each condition. For quantitative analysis of the sarcomere length, a total of 20 images at different ROIs and focus depths were used. Each image contained at least 50 sarcomere lengths and an average value of sarcomere length was first obtained from each image.

Imaging of calcium transients

Tyrode solution was prepared with the following composition (mM): NaCl 134, KCl 2.68, $MgCl_2$ 1.05, $CaCl_2$ 1.80, NaH_2PO_2 0.4, $NaHCO_3$ 12, Glucose 5.56. The pH was adjusted with NaOH to reach 7.4. Spontaneous Ca^{2+} release activity of the hECTs was monitored with Ca^{2+} sensitive fluorescent dye Fluo-4 (10 mM Fluo-4 AM) diluted in Tyrode solution for 45 min near 32 °C. A scientific CMOS camera recorded spontaneous Ca^{2+} transients at 15 frames per second (Thorlabs, CS2100M). Custom Matlab script was used to analyze the video's temporal changes of the fluorescence intensity at different ROIs. The intensity of each frame was normalized to a background baseline recorded without the sample. The calcium transients were recorded from at least three different ROIs per biological replicate and two biological replicates were used for each condition. For the quantitative analysis of the calcium dynamics, a total of 50 transients were used per condition.

Transmitted light optical microscope images

The hECTs were removed from the incubator and placed on a trinocular inverte microscope (AmScope, IN200TB) with 4x magnification. Bright-field videos were recorded at room temperature at 15 frames per second by a CCD camera (FLIR, Grasshopper3 GS3-U3-15S5M) for 10 s. After recording, the hECTs were quickly placed back into the incubator for the next day's recordings.

Dark field microscope

Dark-field images were captured on an inverted optical microscope (Nikon Eclipse Ti-U) equipped with a CCD camera (FLIR, Grasshopper3 GS3-U3-15S5M), a dark-field condenser (Nikon, Ti-DF, NA ~0.8-0.95) and a 40x objective lens (Nikon CFI Super Plan Fluor ELWD, NA = 0.6).

Cross-sectioned hECT slices

The hECTs were fixed by gradually increasing the concentration of paraformaldehyde (2%-4% in 1% increase, 30 min). Then, the fixed hECT was embedded in optimal cutting temperature compound (OCT compound, Fisher scientific, 23-730-571) prior to frozen sectioning by a microtome-cryostat (Leica CM3050S). The 10 µm thick cross-sectioned hECT slides were mounted on tissue glass slides for further imaging. For t-tubule staining, the cross sectioned slices were stained with WGA-Alexa Fluor 488 (Life Technologies, W11261) for 10 min, followed by rinsing in 1xPBS for 5 min.

Nanoindentation measurements

The micromechanical characteristics of cardiac tissues, suspended between two pillars and immersed in tissue culture medium, were assessed using the indentation technique at room temperature (Hyditron Biosoft, Bruker, Billerica, MA). The details were given in the supporting information of a previous report.[1] The hECT and GNR-hECT were tested at 4, 8, 12 and 16 days of culture.

S2. GNR synthesis and characterization

Cetyltrimethylammonium bromide (CTAB) stabilized GNRs were synthesized using a seed mediated growth method as previously described.[2] The chemicals were purchased from Fisher Chemical and Sigma-Aldrich. All solutions were prepared using deionized water (18 Mohm) purchased from Thermo Scientific (AA36645K7). The entire process was performed in a water bath at 30°C. The seed solution consisted of a mixture CTAB (4.7 mL, 0.1 M) and HAuCl4 (25 µL, 50 mM). Then, freshly prepared NaBH4 (300 µL, 10 mM) was added to the mixture under vigorous stirring until the solution become light brown color. The growth solution was prepared with HCl (190 µL, 1M), HAuCl4 (100 µL, 50 mM) and CTAB (10 mL, 0.1 M). The mixture was gently stirred for 5 min. Subsequently, AgNO3 (120 µL, 10 mM) at 4°C was added to the mixture. Then ascorbic acid (100 µL, 100 mM) was added. After thoroughly shaking, the solution was turned to colorless in few seconds. Finally, 24 µL of seed solution was added to 10 mL of the growth solution. The mixed solution was vigorously shaken for 5 sec and left undisturbed for 2 hours at 30°C. The final product GNR-CTAB solution was stored at room temperature for the next step. The SEM image of the CTAB stabilized GNR is shown in Figure S1a and the size estimation is shown in Figure S1b.

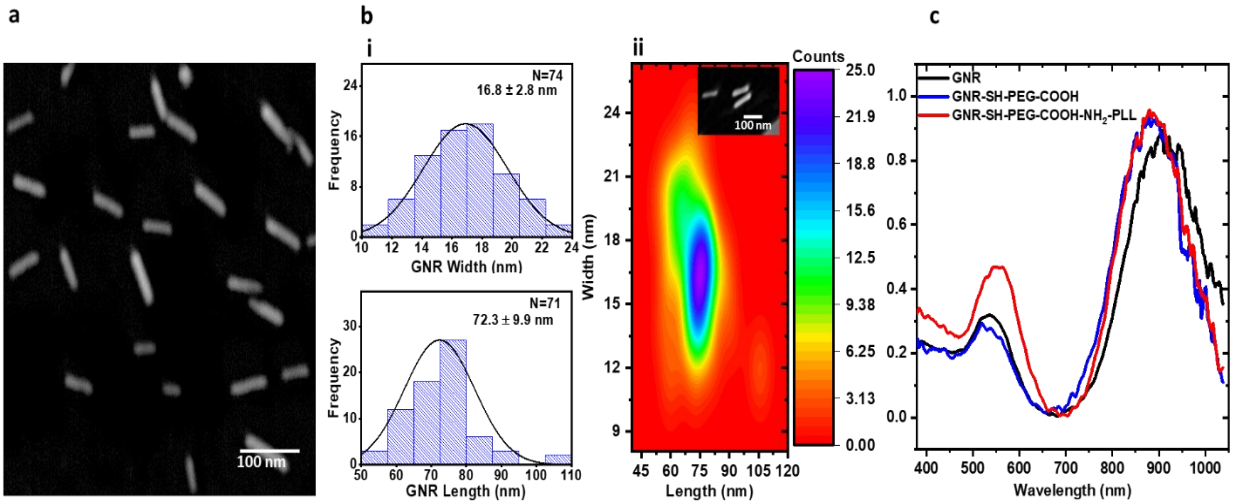

Figure S1. GNR characterization results. (a) SEM image of the CTAB-GNR sample. (b) Size characterization of the CTAB-GNRs based on the SEM images. (i) Length (long axis) and width distributions of the CTAB-GNR sample and (ii) the corresponding size distribution in the heat map format. (c) Extinction spectra of CTAB stabilized GNR (black), after PEG functionalization (step 1, blue) and after PLL functionalization (step 2, red) in 1xPBS solution.

S3. Additional AFM images of fibrin and GNR-fibrin hydrogels.

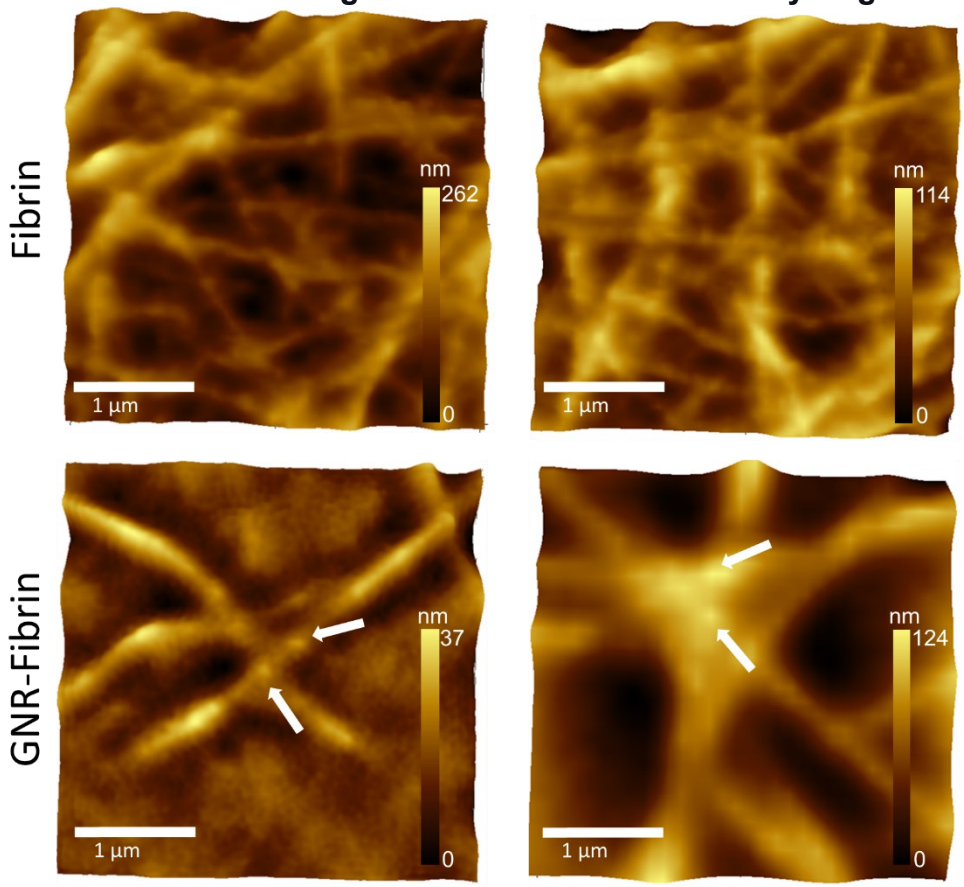

Figure S2. AFM images of fibrin and GNR-fibrin hydrogels. The white arrows indicate the GNRs on the fibrin fibers.

S4. The improved synchronization of calcium transients of a hiPSC-CM 2D layer with the presence of GNR-fibrin.

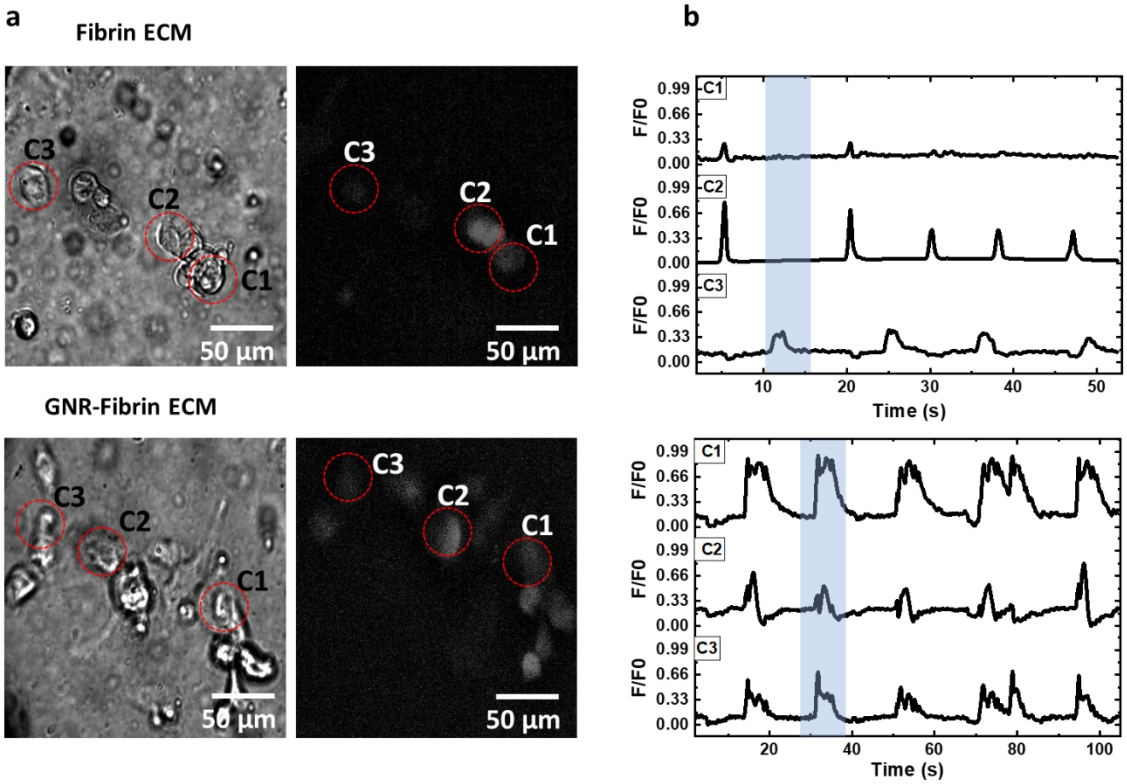

Figure S3. (a) Left panel: bright field optical images of live hiPSC-CMs cultured in fibrin ECM and GNR-fibrin ECM. Right panel: fluorescence images of hiPSC-CMs labeled with Fluo-4. (b) Calcium transients time traces from three different CMs (C1, C2 and C3) at three different locations selected in the fluorescence images in (a).

S5. The formation of 3D hECT in milli-tug construct.

The preparation of both hECTs and GNR-hECTs is depicted in Figure S4a. Remarkable disparities in the internal morphology of the cross-sectioned slides were observed between hECTs and GNR-hECTs on day 16 of culture. Additionally, the presence of GNRs was confirmed through dark field microscope images (refer to Figure S4c).. Due to the low diffusion of the light in the thicker live hECT locations, the dark field images of were obtained at the right edges.

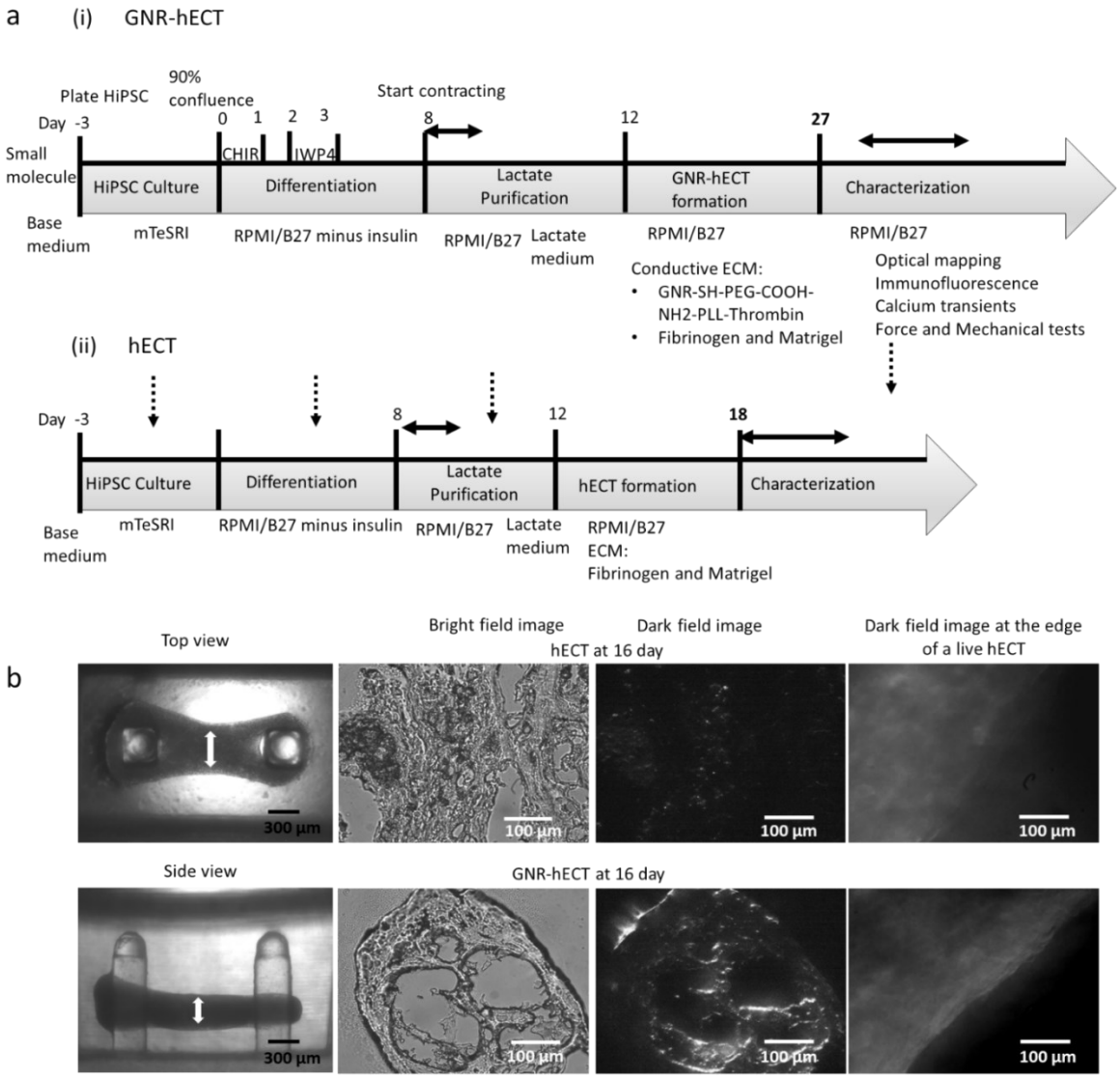

Figure S4. (a) Timelines for the formation and characterization of hiPSC-CMs derived GNR-hECT ((i), top panel) and hECT ((ii), bottom panel). (b) Column 1: top and side views for a hECT at day 16 of culture. The corresponding images for a GNR-hECT are shown in Figure 2b of main text. Column 2-4: the optical microscope images of hECTs at day 16 of culture (top row) and GNR-hECT (bottom row). Column 2: bright field (transmitted light) optical images of the cross-sectioned slides of the tissue. Column 3: dark field microscope

images (Right panel) of the hECT at day 16 of culture. Column 4: dark field images at the edge of a live hECT and GNR-hECT.

S6. Intracellular calcium imaging in the hECT without and with GNR.

We further investigated the intracellular calcium transients within the hECT loaded with Fluo-4 to explore the dynamics of calcium handling. Three different regions were selected, and the concentration of calcium ions was represented as fluorescence intensity (F) of dye divided by the background intensity (F_0). As shown in Figures S5a, on both day 4 and day 11 of culture, the normalized calcium transients from the hECTs manifested a higher variation in the shape compared to the more uniform transients from GNR-hECTs. We defined the duration of the calcium transients by the full width at half maximum (FWHM). As depicted in Figure S5b, a noticeable decrease in the FWHM is observed in hECTs between day 4 and day 11. In contrast, the FWHM of the calcium transients in the GNR-hECTs exhibited an opposite behavior. The results suggest a slow removal of intracellular calcium for the day 11 in GNR-hECts. This condition may generate a high concentration of intracellular calcium, responsibly greater twitch force contraction recorded. The reduction in the FWHM of the calcium transient in hECTs on day 11 might be attributed to the relatively brief lifespan of these tissues. Because of the presence of motion artifacts, we did not analyze the rise and decay time of the calcium transients.

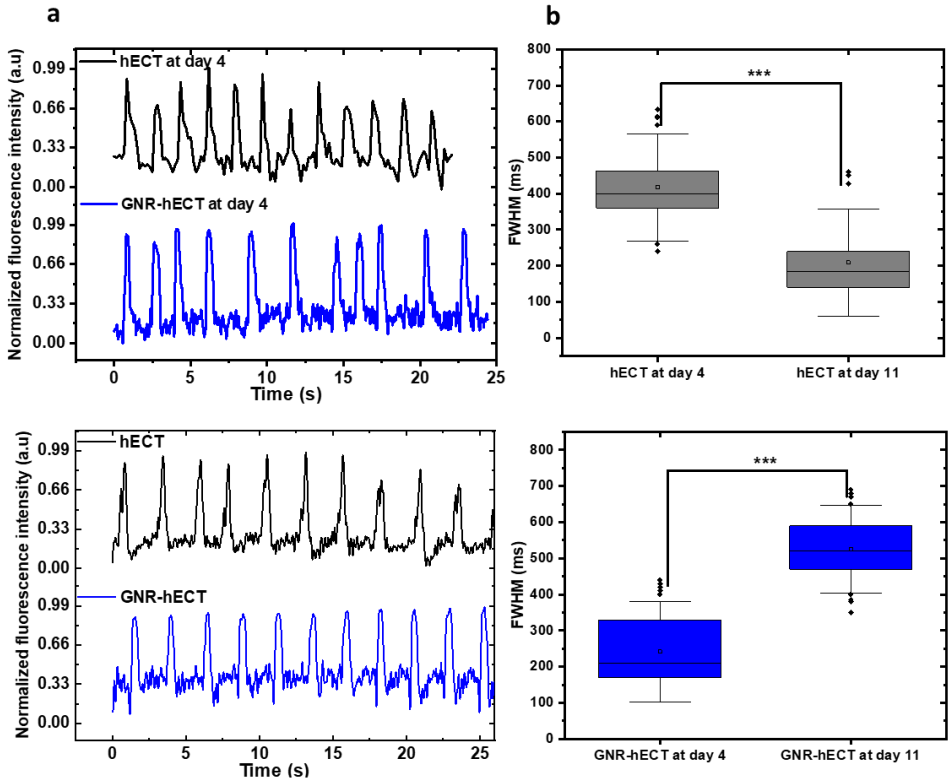

Figure S5. (a) The typical normalized calcium transients from hECTs(black color) and GNR-hECTs (blue color) at day 4 and day 11 of culture. (b) The FWHM of the calcium

transients from tissues at day-4 and day-11 (from two samples per day and three repeats per sample). The error bar is the standard deviation.

S7. Volume nuclei/sarcomere ratio and nuclei count.

We quantified the percentage of sarcomere in the tissue by using the volume nuclei/sarcomere ratio. To calculate this ratio, we processed z-stacks (containing 10 images from the upper layers without voids) of confocal fluorescence images by applying an intensity threshold. This allowed us to determine the occupied areas of both nuclei (stained with DAPI) and sarcomeres (stained with α-actinin) in each image. The volume was then computed by summing the product of the area and the depth between multiple images. As shown in Figures S6a, a significant difference in the nuclei-to-sarcomeres ratio was observed when comparing the volume ratios between hECTs and GNR-hECTs on both day 4 and day 16 of culture. The ratios of GNR-hECTs are obviously lower, suggesting more sarcomere content per CMs in the GNR-hECTs. Furthermore, a notable reduction in the ratio was evident for the GNR-hECTs after 9 months of culture, as shown in Figures S6b.

Additionally, we quantified the number of nuclei within the z-stacks (with the same volume) under analysis. As illustrated in Figures S6c and d, there was no statistical difference in the nuclei number from day 4 to day 16 in both hECTs (Figure S6c) and GNR-hECTs (Figure S6d). Notably, the mean number of nuclei in GNR-hECTs was consistently lower than that in hECTs at both day 4 and day 16. This is consistent with our observation that the GNR-hECT exhibited higher porosity during the early stages. Remarkably, after 9 months of cultivation, the nuclei number in GNR-hECT reveled an obvious increase, indicating a higher cellular density over time.

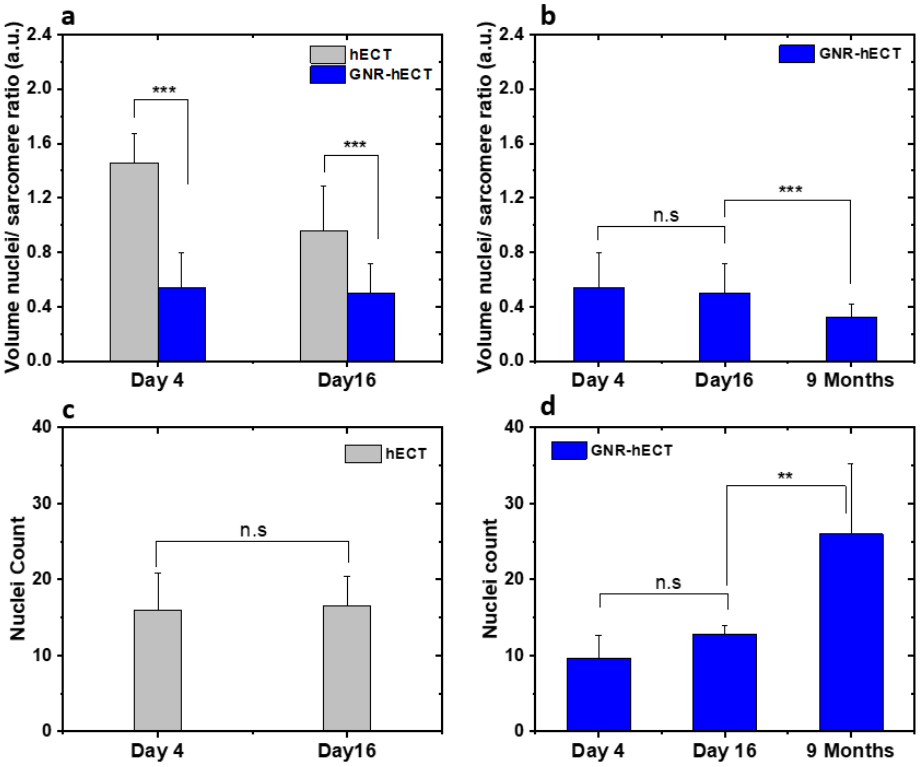

Figure S6. Volume sarcomere ratio of the hECTs with and without GNRs. (a) Comparation of the ratios between hECTs and GNR-hECTs at day 4 and 16 of culture. (b) Comparation of the volume ratios for GNR-hECTs at day 4, 16 and 9-months of culture. The ratios were derived from two samples, each analyzed at three distinct locations. In each z-stack, 10 images were obtained from the upper layers without any voids, with a depth of 0.2 µm between each image. (c) The nuclei number within the analyzed z-stacks of hECTs. (d) Comparison of the nuclei number of GNR-hECTs at day 4, day 16, and after 9 months of culture.

S8. Morphology of the isolated CMs for hECTs at day 16 of culture

To better understand the morphology of individual cells in the tissue, we isolated some cells from tissues on day 16 of culture. The hECTs and GNR-hECTs were dissociated into single cardiomyocytes by using papain-base solution containing 20 U/ml of papain enzyme (Sigma-Aldrich 76220), 1.1 mM EDTA and 5.5 mM l-Cysteine-HCL (Sigma-Aldrich C7880), diluted in 1xEBSS (Gibco 24010-043). The tissues were continuous stirred in papain-base solution at 35°C for 10 min. The papain activity was stopped by adding DMEM (Corning 10013CV) supplemented with 10 % FBS (Gibco 26140079). The solution was centrifuged at 1000 RPM for 5 min at 25 °C. Then, the yielded pellet was resuspended in RPMI/B27 containing insulin, 5 µM Y27632 (Tocris, 1254) and 10% FBS. Cell culture plates were treated with 10 µg ml^{-1} of human fibronectin (Gibco 33016-015) for 1 hr at 35°C and rinsed with sterile 1xPBS. The isolated CMs were replanted on the fibronectin coated cell culture plate with fibronectin and stored in a cell culture incubator (37°C, 5%, CO2, 90% humidity) before measurements.

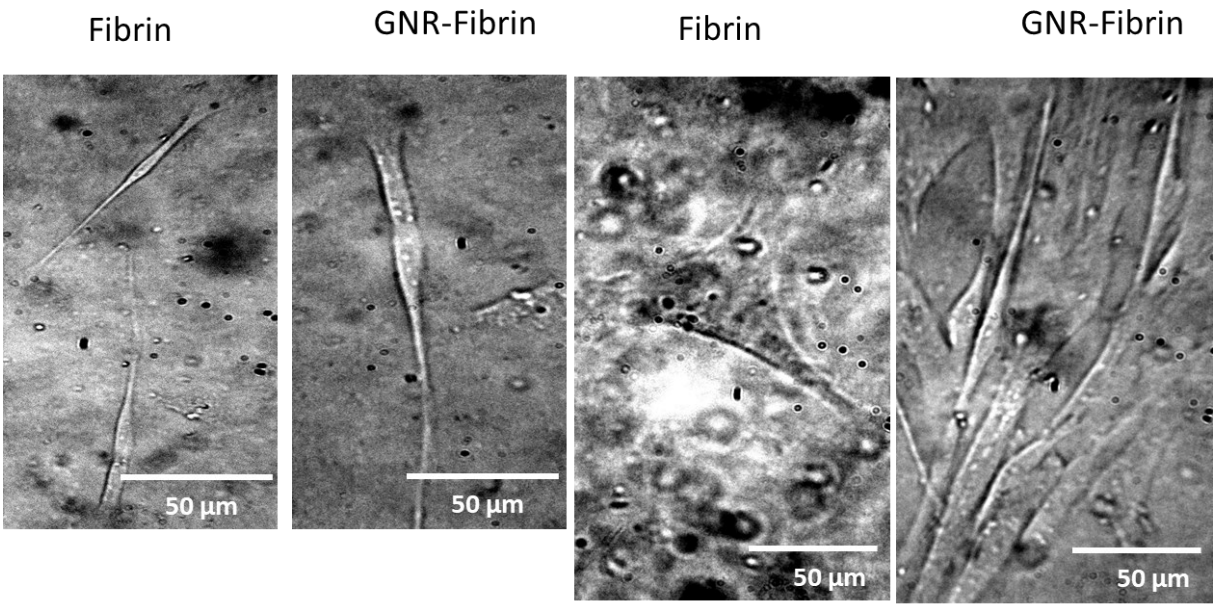

Figure S7. The bright-field images of cells isolated from hECTs at day 16 of culture. Cells obtained from hECTs exhibited a wider range of geometrical shapes, while those from GNR-hECTs displayed a more uniform and elongated shape, resembling adult CMs.

S8. Tissue stiffness

We employed indentation measurements (see details in S1) to study the evolving mechanical properties of hECTs as a function of culture time. A side-view image of the indentation probe on the hECT in the milli-tug construct is shown in Figure S8a. Based on the load-displacement curve, we calculated the elastic modulus (Young's modulus) of the tissues at different culture days. The results are shown in Figure S8b. The elastic modulus of hECTs and GNR-hECTs exhibited in the ranges of 4.3-7.2 kPa and 5.6-11.6 kPa, respectively. Previous studies on ECTs containing CMs and endothelial cells have reported a Young's moduli around 4-5 kPa.[3] Interestingly, GNR-hECTs consistently exhibited higher mean elastic modulus, although statistical significance was only achieved at day 16 of culture due to substantial sample-to-sample fluctuations. Furthermore, the relationship between culture time and elastic modulus wasn't monotonic. We observed an initial increase from 4 to 8 days, followed by a decrease on day 12, and then another increase on day 16 of culture. This trend is consistent with the twitch force results in Figure 4D, suggesting a possible link between mechanical properties and contractile function. Similar results have been observed in our previous studies.[1] In the future studies, long-term studies are necessary to investigate whether GNR-hECT stiffness converges towards native myocardium.

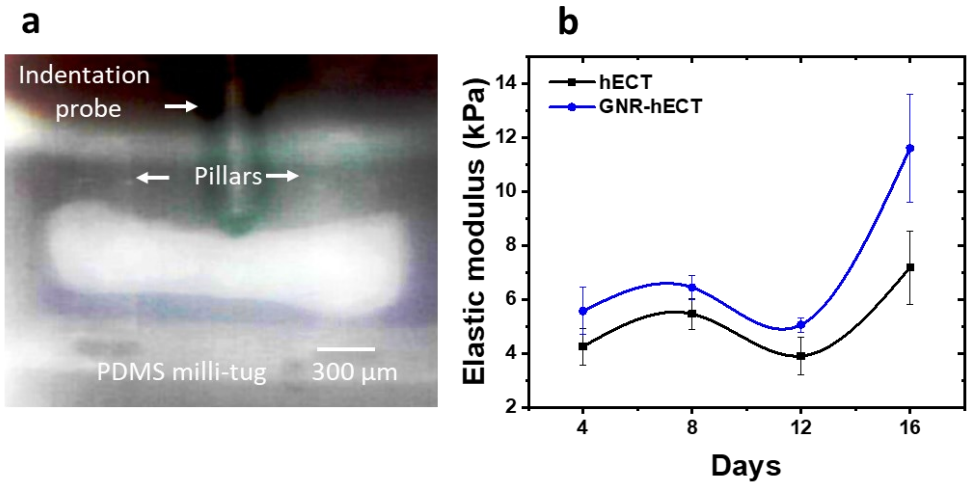

Figure S8. Indentation measurements of the hECTs and GNR-hECTs. (a) Side-view bright field image of a GNR-hECT under the indentation probe at day 16 of culture. (b) Elastic modulus of the tissues as a function of culture time. The error bars are calculated from three samples per condition, with each sample measured in triplicate. Significative differences were found at day 16 of culture.

References

1. A. Sesena-Rubfiaro, N. J. Prajapati, L. Paolino, L. Lou, D. Cotayo, P. Pandey, M. Shaver, J. D. Hutcheson, A. Agarwal and J. He, *ACS Biomaterials Science & Engineering*, 2023, **9**, 1644-1655.
2. L. Scarabelli, A. Sánchez-Iglesias, J. Pérez-Juste and L. M. Liz-Marzán, *The Journal of Physical Chemistry Letters*, 2015, **6**, 4270-4279.
3. H. Masumoto, T. Nakane, J. P. Tinney, F. Yuan, F. Ye, W. J. Kowalski, K. Minakata, R. Sakata, J. K. Yamashita and B. B. Keller, *Scientific Reports*, 2016, **6**, 29933.